Computational Materials Science 97 (2015) 127–135

Contents lists available at ScienceDirect

Computational Materials Science

journal homepage: www.elsevier.com/locate/commatsci

Effect of Re on dislocation nucleation from crack tip in Ni by atomistic simulation

Zheng-Guang Liu [a,d], Chong-Yu Wang [a,b,c,*], Tao Yu [a]

[a] Central Iron and Steel Research Institute, Beijing 100081, China
[b] Department of Physics, Tsinghua University, Beijing 100084, China
[c] International Centre for Materials Physics, Academia Sinica, Shenyang 110016, China
[d] Department of Physics, North University of China, Taiyuan 030051, China

ARTICLE INFO

Article history:
Received 5 March 2014
Received in revised form 3 July 2014
Accepted 13 August 2014

Keywords:
Dislocation nucleation
Crack
Molecular dynamics
Re

ABSTRACT

The effect of Re on the dislocation nucleation from a crack tip in Ni is investigated using the climbing image nudged elastic band method with a Ni-Al-Re embedded-atom-method potential. The activation energy and frequency of dislocation nucleation are calculated. Calculation results show that the activation energy decreases with Re addition. The decrease of activation energy may be related to the expansion of local structure around the Re atom when dislocation goes through the Re atom. The calculations also show that the frequency of dislocation nucleation can be improved with the Re addition at 300 or 1500 K, which means that the ductility of crack in Ni may be enhanced by Re.

1. Introduction

Re is a crucial heavy element in Ni-based single-crystal superalloys, and the fracture strength of superalloys can be markedly improved by Re addition [1–3]. However, the effect of Re on the ductility of crack in superalloys has not been well explored yet. The ductility of crack is closely related to the dislocation nucleation from crack tip. The dislocations nucleated usually cause the crack-tip blunt and the plastic deformation at crack tip. Some experiments have demonstrated that cracks often appear in the γ(Ni) matrix phase or γ(Ni)/γ'(Ni_3Al) phase interface of Ni-based single-crystal superalloys [4–6]. It is needful to explore the effect of Re on dislocation nucleation from crack tip in γ(Ni) matrix.

Several studies have been devoted to the topic (dislocation nucleation from crack). Rice [7] analyzed the dislocation nucleation to evaluate brittle versus ductile responses at a crack tip, based on the Peierls concept. Rice and Beltz [8] gave an analytical expression for the activation energy of the dislocation nucleation at a 2D crack. Zhang et al. [9] gave a critical stress intensity factor for dislocation emission from an atomistic crack tip under mode II loading based on molecular dynamics (MD) simulations in Cu. Using the MD method, Hess et al. [10] reported that the temperature and crystal orientation have an important influence on dislocation nucleation from a crack tip in Ni. Zhu et al. [11] reported the first atomistic calculation of the activation energy for the nucleation of a 3D dislocation loop from a stressed crack tip in a single crystal of Cu, using the nudged elastic band (NEB) method. Gordon et al. [12,13] studied the activation pathways for dislocation loop nucleation from crack tips in α-Fe based on the NEB method, concluding that substitutional solutes have an important influence on the activated process of nucleating dislocation.

The reason that activation energy of dislocation nucleation is changed by alloy addition needs to be explored. Rice [7], Rice and Beltz [8], Zhu et al. [11], and Xu et al. [14] indicated that a larger displacement vertical to the slip plane has the effect of reducing resistance to and activation energy of dislocation nucleation. Gordon and Neeraj [13] suggested that the bond strength between the "hardening" solute and Fe can describe the solute influence on the activation energy of dislocation nucleation. We speculate that the activation energy of dislocation nucleation may also be related to the local structure expansion surrounding the solute atom, and this relation is explored in the present work.

In the present work, the effect of Re on the dislocation nucleation from a crack tip in Ni, including the activation energy and frequency of dislocation nucleation, is investigated using the climbing image nudged elastic band (CI-NEB) method [15–17] with a Ni-Al-Re embedded-atom-method (EAM) potential [18]. This potential has been applied to predict the effect of Re on the dislocation and crack in Ni or Ni/Ni_3Al interface [18–20].

* Corresponding author at: Department of Physics, Tsinghua University, Beijing 100084, China. Tel.: +86 01062772782.
E-mail addresses: guang212@163.com (Z.-G. Liu), cywang@mail.tsinghua.edu.cn (C.-Y. Wang), ytao012345@163.com (T. Yu).

http://dx.doi.org/10.1016/j.commatsci.2014.08.030
0927-0256/

2. Modeling and procedures

2.1. Model for the activation energy of dislocation nucleation from crack tip

In the computational model for the activation energy (ΔE_{dis}) of dislocation nucleation from crack tip, the mode I (tensile) $(\bar{1}\,1\,1)[1\,0\,1]$ crack at the stress intensity factor K_I is constructed by the anisotropic linear elastic continuum solution [21]. This model follows a published description [11], but with some modifications to the crack system (Fig. 1). The upper and lower atomic layers across the $(1\,1\,\bar{1})$ slip plane (Fig. 2) are the nucleation site of the Shockley partial dislocation with $b = a_0/6[\bar{1}\,2\,1]$. The crack surface is a $(\bar{1}\,1\,1)$ plane, and the crack front is oriented along the $[1\,0\,1]$ direction. The crack tip lies in the center of a cylinder with radius R = 90 Å. The total number of atoms in the system is 138,336. The atoms within 10 Å of the outer surface are fixed according to a prescribed boundary condition, during the MD relaxation, whereas all remaining atoms are free to move. The cylinder axis, along the $[1\,0\,1]$ direction, consists of 24 unit cells with a total length of about 59.7 Å (it is longer than 40 b, sufficient to obtain an accurate value for the activation energy of an isolated dislocation loop [14], and b is the value of Burgers vector $b = a_0/6\langle 1\,1\,2\rangle$ of a Shockley partial dislocation, where a_0 = 3.52 Å is the lattice constant of Ni). As the dislocation emits spontaneously in the $(\bar{1}\,1\,1)[1\,0\,1]$ crack system for an atomically sharp crack tip in Ni (the similar case takes place in Cu [11]), one layer of atoms behind the crack tip is removed to generate a stable, but slightly blunted crack. In practice, there are many sorts of cracks in materials, and here, only the crack system in which the dislocation nucleation takes place easily is considered.

The loading scheme is performed in increments of $0.01K^G_{th}$ from a stress intensity $K_I = 0.60K^G_{th}$ until the dislocation emission occurs at $K_I = 0.85K^G_{th}$. Here, K^G_{th} is the theoretical Griffith stress intensity factor. Next, the unloading scheme is performed in decrements of $0.01K^G_{th}$ from $K_I = 0.85K^G_{th}$ to $K_I = 0.60K^G_{th}$. The emitted dislocation is not found to disappear during unloading. Thus, there are two system states at each stress intensity factor when $K_I < 0.85K^G_{th}$. The two system states are the initial and final states of the pathway for the activated process of dislocation emission. The initial state is produced during loading, but dislocation emission does not occur; the final state is produced during unloading, and dislocation emitted occurs. The initial and final states have the same outer boundary since the same stress intensity factor is applied to both the initial and final states.

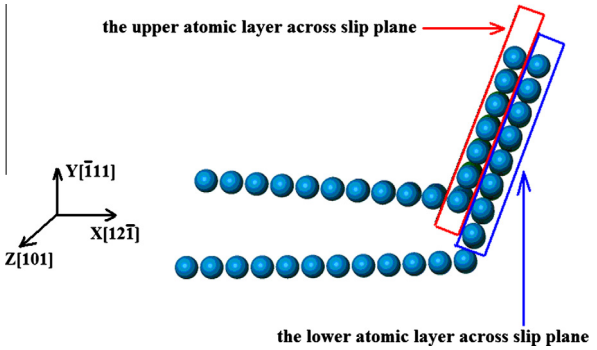

Fig. 2. Upper and lower atomic layers across the $(1\,1\,\bar{1})$ slip plane near the crack tip.

After getting the initial and final states of the pathway for dislocation emission at a given load K_I ($< 0.85K^G_{th}$), the CI-NEB method is used to determine the minimum energy path (MEP) of a partial dislocation loop bowing out from the initially straight crack front. The activation energy (ΔE_{dis}) for the dislocation loop nucleation is obtained as well. The state with the highest energy along the MEP is the saddle-point state. The activation energy (ΔE_{dis}) is the energy difference between the saddle-point state and the initial state. The calculation is considered to have converged when the potential force on each replica vertical to the path is less than 0.005 eV Å^{-1}.

The CI-NEB calculation is carried out through a classical molecular dynamics code (LAMMPS) and performed in two stages [22]. In the first stage, the general NEB calculation [15] is performed, i.e., the set of replicas (generated between the initial and final states) converge toward the MEP of conformational states that transition over the barrier. The replica states are roughly equally spaced along the MEP due to the inter-replica spring force. In the second stage, the barrier–climbing calculation [16] is performed, i.e., the replica with the highest energy is selected and the inter-replica force on it are converted to a force that drives its atom coordinates to the top or saddle point of the barrier. And the other replicas rearrange themselves along the MEP so as to be roughly equally spaced. When both stages are completed successfully, one of the replicas should be the saddle point, and the activation energy can be obtained using the few replicas.

In the calculations of the activation energy (ΔE_{dis}) and frequency (ν) of dislocation nucleation, two schemes for Re addition are designed. In the first scheme, a single Re atom is placed in the lower or upper atomic layer of the slip plane. In the second scheme,

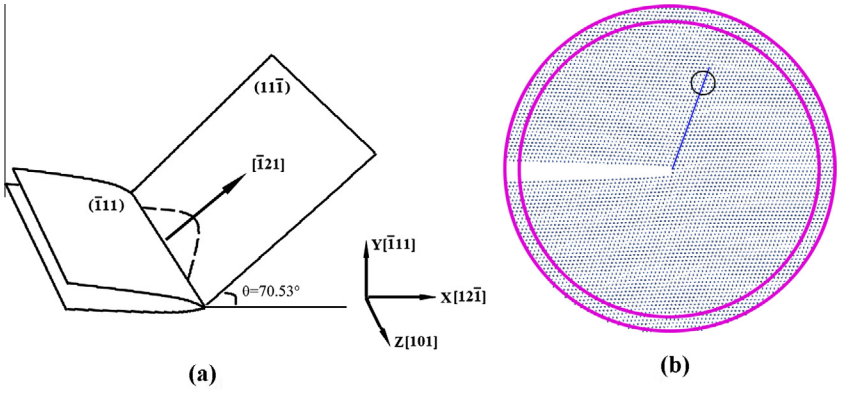

Fig. 1. (a) Sketch map of $(\bar{1}\,1\,1)[1\,0\,1]$ crack system with the $(1\,1\,\bar{1})$ slip plane. The arc-shaped dashed line is the dislocation loop in the $(1\,1\,\bar{1})$ slip plane. The Burgers vector of the dislocation loop is $b = a_0/6[\bar{1}\,2\,1]$; (b) atomic configuration of side view for $(\bar{1}\,1\,1)[101]$ crack system. The black circle presents the location of dislocation core. The region between two pink circles presents the outer boundary of crack model. (For interpretation of the references to color in this figure legend, the reader is referred to the web version of this article.)

3 or 6 at.% Re is randomly doped over the whole system, following experimental observations that the Re atoms tend to distribute randomly over the Ni matrix of Ni-based single-crystal superalloys and are not prone to clustering [23,24]. In the analysis presented below, only the calculated results for ΔE_{dis} and v in one sample for 3 and 6 at.% Re random distribution are given, but this has no influence on the discussion.

2.2. Model for the Peierls stress calculation with and without Re atom

Dislocation mobility sometimes decreases when an impurity is added because the impurity can servers as obstacle for dislocation motion. The effect of Re on dislocation mobility may be different from that on the energy barrier of dislocation nucleation from crack tip. In this subsection, to explore the effect of Re on dislocation mobility, the approximate Peierls stress [25] is calculated for Ni matrix with and without Re atom. Here, the approximate Peierls stress is the minimum stress required to make a straight dislocation move at zero temperature [26].

In the computational model for the Peierls stress of dislocation mobility, a Ni bulk including two Shockley partial dislocations is constructed (Fig. 3). The model follows a published description [27], but with some small modifications in our calculation. There are 298.8 Å along the $x[\bar{1}0\bar{1}]$ direction, 109.8 Å along the $y[1\,1\,\bar{1}]$ direction, and 276.0 Å along the $z[1\,\bar{2}\,\bar{1}]$ direction. Periodic boundary conditions are used in the x and z directions, but a free boundary condition for the y-direction. The two Shockley partial dislocations can be produced in the procedure: an edge dislocation with Burgers vector $b = a_0/2[\bar{1}0\bar{1}]$ is placed in the center of the bulk firstly. The bulk is then relaxed, and the edge dislocation is dissociated to two Shockley partial dislocations in the $(1\,1\,\bar{1})$ slip plane. The Burgers vectors of two Shockley partial dislocations are $b_1 = a_0/6[\bar{1}\,\bar{1}\,2]$ and $b_2 = a_0/6[\bar{2}\,1\,\bar{1}]$, respectively. Then, we focus on the effect of Re on the mobility of dislocation with $b_1 = a_0/6[\bar{1}\,\bar{1}\,2]$, and calculate the approximate Peierls stress (the minimum stress required to make the straight dislocation with $b_1 = a_0/6[\bar{1}\,\bar{1}\,2]$ move at zero temperature) without and with Re addition. Here, the effect of Re on the mobility of dislocation with $b_2 = a_0/6[\bar{2}\,1\,\bar{1}]$ is not explored since the two Shockley partial dislocations with $b_1 = a_0/6[\bar{1}\,\bar{1}\,2]$ and $b_2 = a_0/6[\bar{2}\,1\,\bar{1}]$ are similar and symmetric.

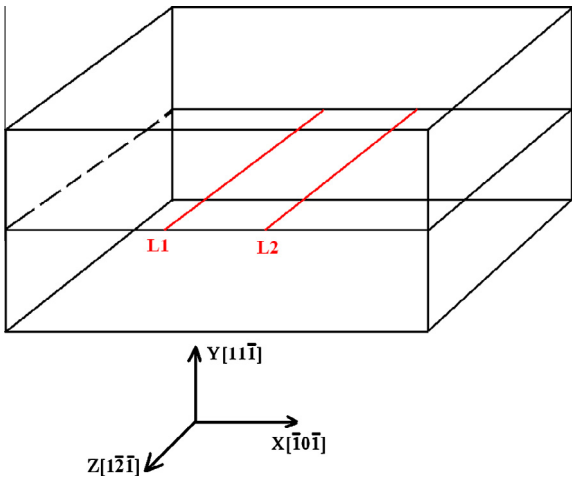

Fig. 3. Two Shockley partial dislocations in a Ni bulk. The red lines "L1" and "L2" represent the dislocation lines with Burgers vectors $b_1 = a_0/6[\bar{1}\,\bar{1}\,2]$ and $b_2 = a_0/6[\bar{2}\,1\,\bar{1}]$, respectively. (For interpretation of the references to color in this figure legend, the reader is referred to the web version of this article.)

To calculate the Peierls stress, the external force is applied, parallel to the $x[\bar{1}0\bar{1}]$ direction, to each atom in the upper and lower surfaces in the $y[1\,1\,\bar{1}]$ direction. The intensity of the force is proportional to the inverse of the number of atoms in the surface, in order to make sure the force per unit area is the same (with opposite sign) in the upper and lower surfaces. When the dislocation with $b_1 = a_0/6[\bar{1}\,\bar{1}\,2]$ begins to move, the approximate Peierls stress can be obtained according to the external force applied to the upper and lower surfaces.

To evaluate the effect of Re on the mobility of dislocation, two schemes for Re addition are designed. In the first scheme, a single Re atom is placed in (or ahead of) the dislocation line with $b_1 = a_0/6[\bar{1}\,\bar{1}\,2]$. Here, "in (or ahead of) the dislocation line" means that Re atom is placed in (or in the left of) the red line "L1" in Fig. 3. In the second scheme, 3 or 6 at.% Re is randomly doped over the whole Ni bulk.

3. Results and discussion

3.1. Influence of Re on ΔE_{dis}

First, to visualize the dislocation nucleation from a crack tip, the configurations of the initial, saddle-point, and final states (Fig. 4) were obtained by calculating ΔE_{dis}, with $K_I = 0.64K_{th}^G$ and a single Re atom in the $(1\,1\,\bar{1})$ slip plane. A dislocation loop with Burgers vector $b = a_0/6[\bar{1}\,2\,1]$ is forming at the saddle-point state in Fig. 4(b). Accordingly, the distribution of shear displacement in the $[\bar{1}\,2\,1]$ direction across the two adjacent $(1\,1\,\bar{1})$ slip planes before, near, and past the saddle-point states is produced in Fig. 5. The dislocation loop near the saddle-point state is present in Fig. 5(b). The relative shear slip distances (inside the dislocation loop) between the upper and lower atom layers are bigger than $b/2$; outside the dislocation loop, the relative shear slip distances are smaller than $b/2$. Similar figure has been seen in the literature [11]. In addition, from Fig. 5, the shear displacement near the Re atom is smooth, and the relative shear slip distance is independent of the addition of Re.

From the MEPs for nucleating a dislocation loop from crack tip at $K_I = 0.64K_{th}^G$ and $K_I = 0.82K_{th}^G$, with or without a single Re atom in the $(1\,1\,\bar{1})$ slip plane (Fig. 6), ΔE_{dis} decreases with the addition of Re, but is found to decrease considerably in comparing $K_I = 0.64K_{th}^G$ with $K_I = 0.82K_{th}^G$. At $K_I = 0.64K_{th}^G$, ΔE_{dis} decreases by 3% (from 5.30 to 5.13 eV) with single Re atom addition, while 57% (from 0.21 to 0.09 eV) at $K_I = 0.82K_{th}^G$. The decrease in ΔE_{dis} is sufficient to produce an obvious increase in the nucleation frequency of dislocation. In Section 3.3, the effect of Re on the dislocation nucleation frequency is evaluated.

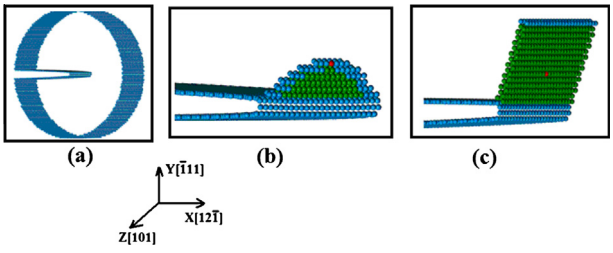

Fig. 4. Initial (a), saddle-point (b), and final (c) configurations obtained by the calculation of ΔE_{dis}, with $K_I = 0.64K_{th}^G$ and a single Re atom in the lower atomic layer of the $(11\bar{1})$ slip plane. The red ball is Re atom, and the other balls are Ni atoms. The green balls represent the hexagonal closed-packed (HCP) atoms. The blue balls around the HCP region consist of a dislocation loop with the Burgers vector $b = a_0/6[\bar{1}\,2\,1]$. (For interpretation of the references to color in this figure legend, the reader is referred to the web version of this article.)

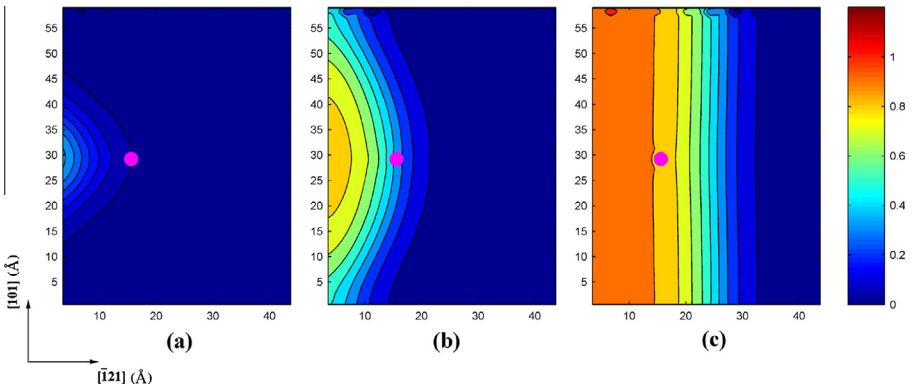

Fig. 5. Contour maps of the shear displacement before (a), near (b), and past (c) the saddle-point states in the $[\bar{1}\,2\,1]$ direction across two adjacent $(1\,1\,\bar{1})$ slip planes, at $K_I = 0.64K_{th}^G$, with a single Re atom in the lower atomic layer of the slip plane, by the CI-NEB calculation. The pink circle marks the position of Re atom. Here, the shear displacement has been normalized by $b = a_0/6[\bar{1}\,2\,1]$. (For interpretation of the references to color in this figure legend, the reader is referred to the web version of this article.)

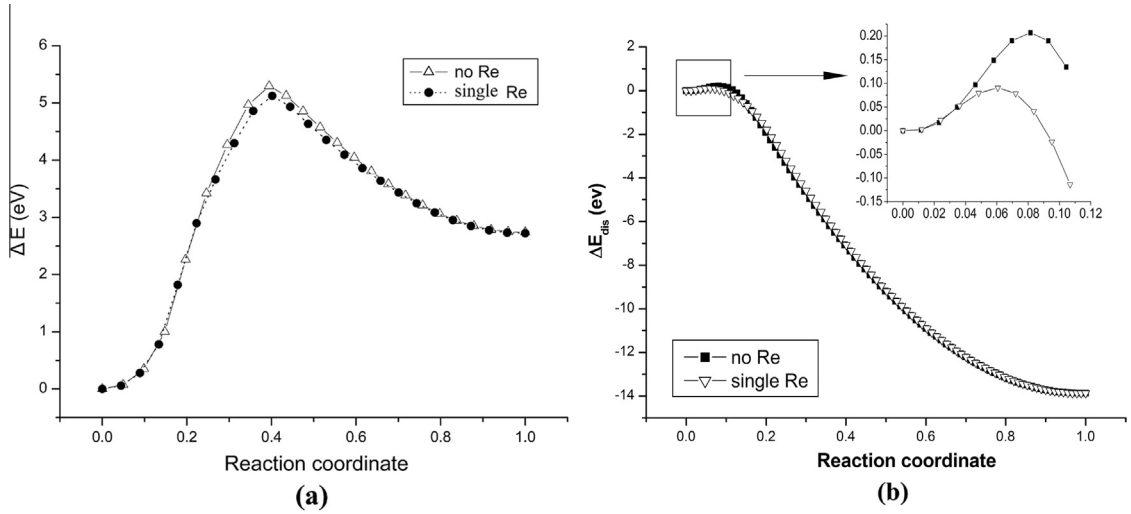

Fig. 6. MEPs for nucleating a dislocation loop from the crack tip, with or without a single Re atom in the $(1\,1\,\bar{1})$ slip plane: (a) at $K_I = 0.64K_{th}^G$; (b) at $K_I = 0.82K_{th}^G$. The energy at the initial state is taken as reference. The normalized reaction coordinate is defined as the ratio between l, the hyperspace arc length along the MEP from the initial state to current state, and l_0, the total arc length along the MEP [11].

Table 1
Activation energy (ΔE_{dis}) of dislocation nucleation.

		0 at.% Re	1 Re atom	3 at.% Re	6 at.% Re
ΔE_{dis} (eV)	$K_I = 0.64K_{th}^G$	5.30	5.13	4.75	4.84
	$K_I = 0.67K_{th}^G$	3.89	3.71	3.30	3.24
	$K_I = 0.77K_{th}^G$	0.90	0.80	0.54	0.47
	$K_I = 0.82K_{th}^G$	0.21	0.09	0.01	0

Table 1 lists the calculated results of ΔE_{dis} corresponding to the addition of 0 at.%, single Re atom, 3 at.%, and 6 at.% Re. For the single Re atom addition, only the calculated results with the Re atom in the lower atomic layer of the slip plane are shown in Table 1, because ΔE_{dis} changes little when the Re atom is in the lower atomic layer. From Table 1, ΔE_{dis} clearly decreases more when the Re concentration in the system increases. (There is an abnormal data point in Table 1 in that ΔE_{dis} at $K_I = 0.64K_{th}^G$ with the addition of 6 at.% Re is larger than ΔE_{dis} with the addition of 3 at.% Re. This arises because the actual number of Re atoms in the dislocation loop with the random addition of 6 at.% Re is lower than that with the random addition of 3 at.% Re, although the value of the former is higher than the latter.)

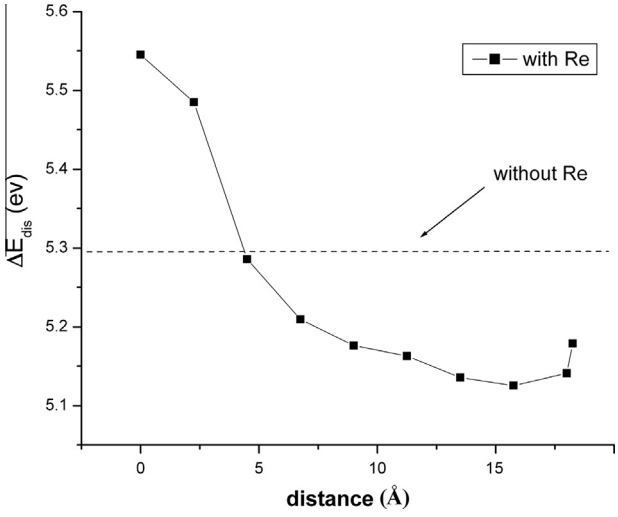

Fig. 7. Variation in energy barrier with the distance between crack tip and single Re atom at $K_I = 0.64K_{th}^G$. The dashed line represents the energy barrier without Re addition.

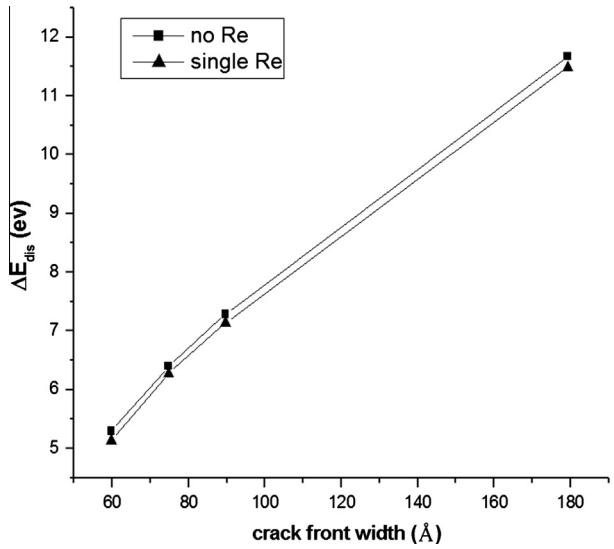

Fig. 8. The variations in energy barriers with lengths of crack front, without and with a single Re addition at $K_I = 0.64K_{th}^G$.

ΔE_{dis} does not always decrease when the Re atom is doped at different sites of the slip plane. ΔE_{dis} can decrease when the Re atom is doped on most sites slightly far from the crack tip. The variation in energy barrier with the distance between crack tip and single Re atom at is depicted in Fig. 7. From Fig. 7, we can find that ΔE_{dis} is smallest when the distance between the Re atom and the crack tip is 15.75 Å. The reason is that the dislocation loop at the saddle-point state just passes through the Re atom which is about 9–16 Å from the crack tip, and this decreases ΔE_{dis}.

In addition, Fig 3(b) shows that the dislocation nucleation at saddle point spans the entire crack front width. To check the convergence of ΔE_{dis} over crack front width, we run NEB calculations for wider crack tip front (74.7 Å, 89.6 Å, and 179.2 Å). Fig. 8 show the variations in energy barriers with lengths of crack front, without and with a single Re addition. It can be seen from Fig. 8 that ΔE_{dis} increases almost linearly with the crack front width, and the value of ΔE_{dis} per unit width of crack front without and with Re addition is approximately equal to 0.065 eV/Å and 0.064 eV/Å, respectively. The result is reasonable. The activation of dislocation nucleation should be more difficult when the dislocation line length (namely, the crack front width) becomes larger, and the activation energy of whole dislocation line should be larger since

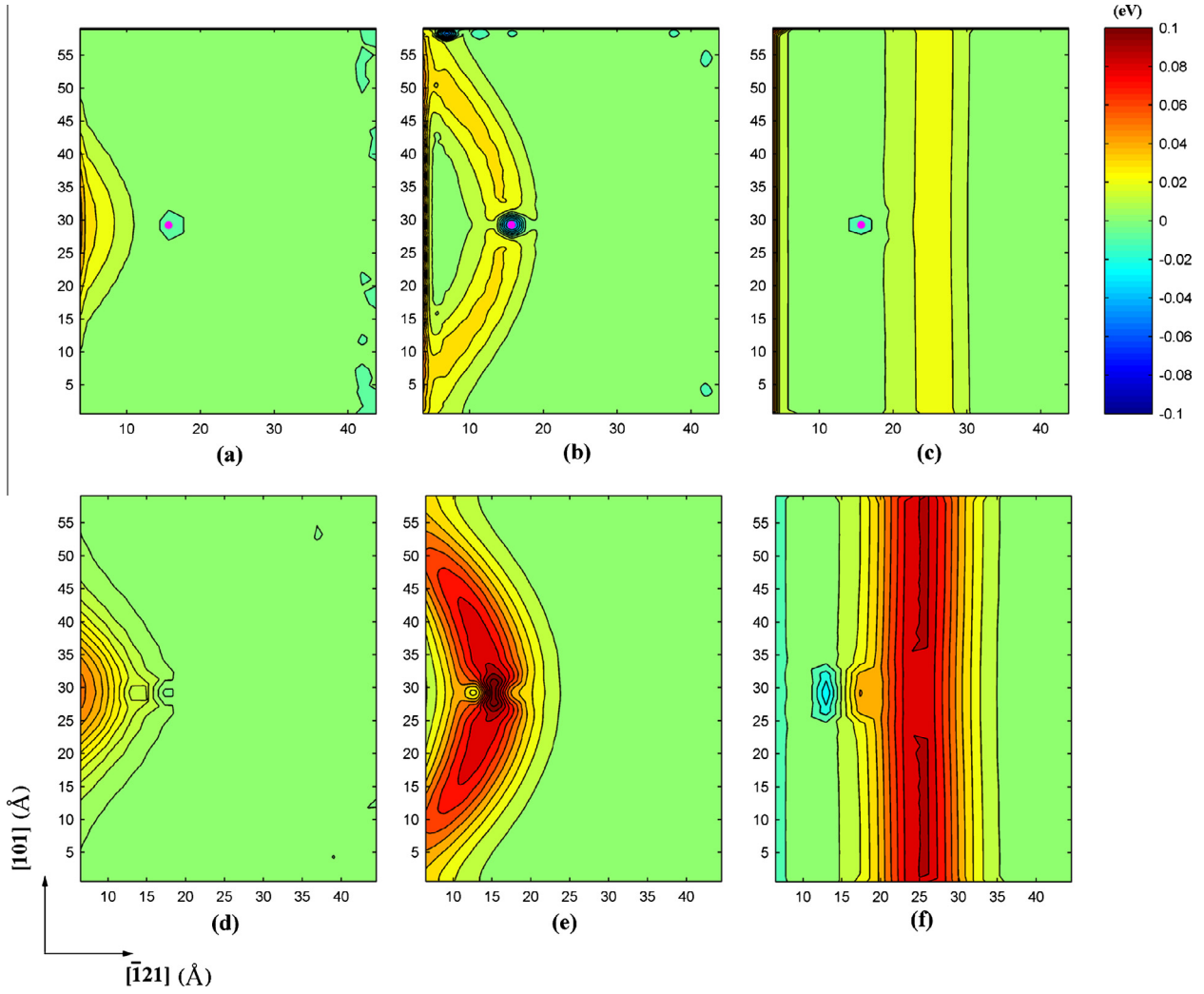

Fig. 9. Contour maps of the energy difference of each atom in the lower (a–c) and upper (d–f) atomic layers across the $(1\,1\,\bar{1})$ slip plane near the crack tip, with $K_I = 0.64K_{th}^G$ and a single Re atom in the lower atomic layer of the slip plane. The pink circle marks the position of Re atom. (a–c) represent the energy differences in the lower atomic layer before, near, and past the saddle-point state in that order; similarly, (d–f) represent the energy differences in the upper atomic layer. (For interpretation of the references to color in this figure legend, the reader is referred to the web version of this article.)

the dislocation nucleation at saddle point spans the entire crack front width.

3.2. Reason that ΔE_{dis} decreases with the addition of Re

The reason that ΔE_{dis} decreases with the addition of Re is that the energy differences of both the Re atom and atoms (near Re atom) decrease. The energy difference of atom j can be written as follows:

$$\Delta E_j^{ti} = E_j^t - E_j^i, \tag{1}$$

where E_j^i is the energy of atom j at the initial state; E_j^t is the energy of atom j at the t state. If the t state is the saddle-point state, ΔE_{dis} can be given:

$$\Delta E_{dis} = \sum_{j=1}^{N} (\Delta E_j^{ti}), \tag{2}$$

where N is the total number of atoms in the whole system. From expressions (1) and (2), ΔE_{dis} is the sum of the energy difference of each atom.

Fig. 9 shows contour maps of the energy difference of each atom in the lower and upper atomic layers across the $(1\,1\,\bar{1})$ slip plane near the crack tip, with $K_I = 0.64K_{th}^G$ and a single Re atom in the lower atomic layer. In the lower atomic layer near the saddle-point state (Fig. 9(b)), the dislocation loop goes through the Re atom, and the energy differences of atoms, which are less than 2.6 Å from Re atom, are smaller compared with those of atoms far from Re atom. In contrast, in the upper atomic layer near the saddle-point state (Fig. 9(e)), no obvious decrease in the energy difference of atoms near Re atom is found. Thus, the overall energy differences for both the Re atom and atoms (near Re atom) in both the lower and upper atomic layers decrease, when the Re atom is added in the lower atomic layer.

When a single Re atom is added in the upper atomic layer of the slip plane, the obvious change of the energy difference of atoms near Re atom is not found.

When 3 or 6 at.% Re is randomly doped into the whole crack system, it is found that the energy differences of atoms near Re atoms near the slip plane are lower compared with the energy differences of atoms far from Re atoms. Fig. 10 shows the contour map of energy difference of each atom in the upper and lower atomic layers across $(1\,1\,\bar{1})$ slip plane near crack tip, with $K_I = 0.64K_{th}^G$ and 3 at.% Re addition in the whole crack system. In Fig. 10(b), in the lower atomic layer of slip plane near the saddle-point state, the energy differences of atoms near Re atoms

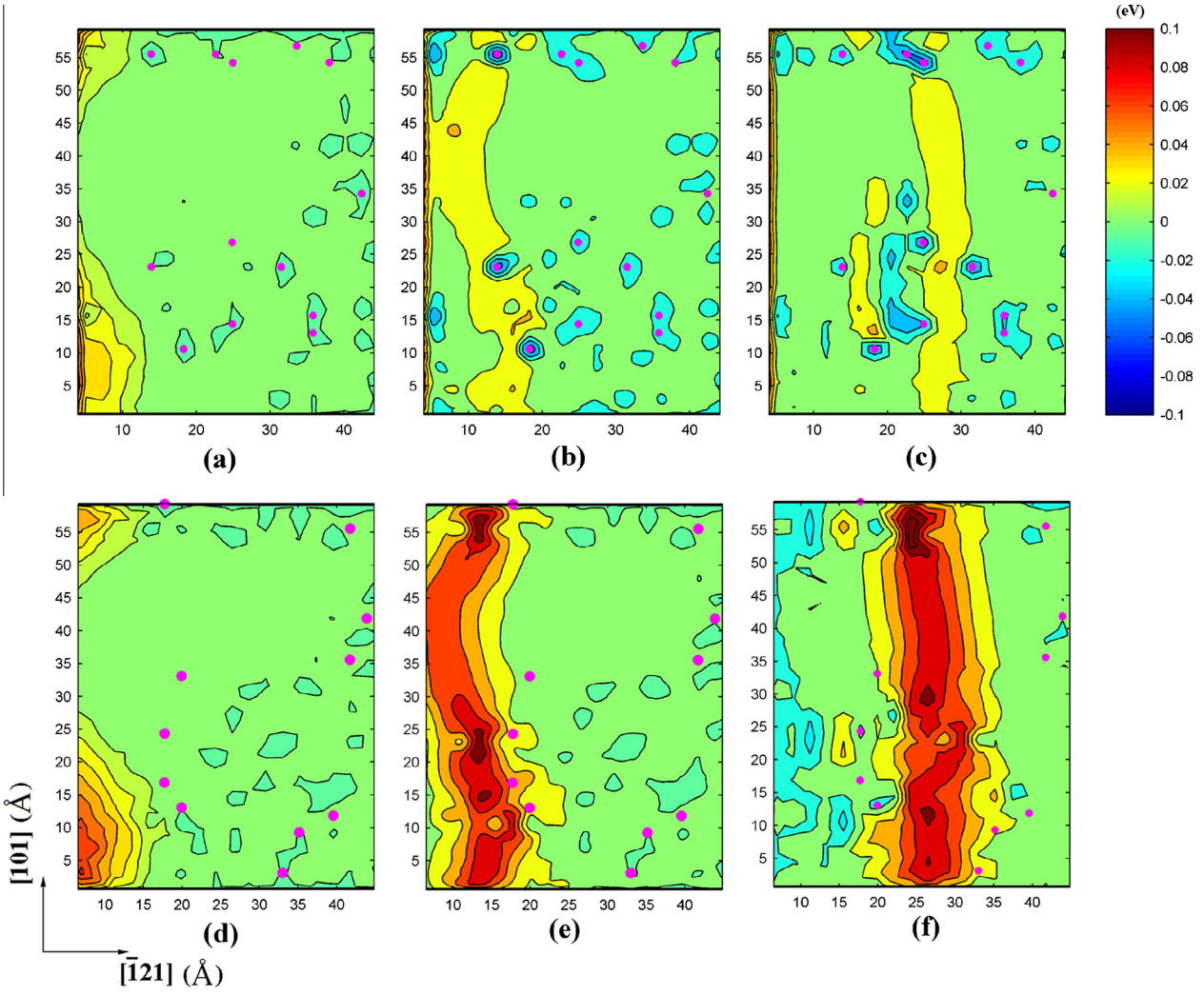

Fig. 10. Contour maps of the energy difference of each atom in the lower (a–c) and upper (d–f) atomic layers across the $(1\,1\,\bar{1})$ slip plane near the crack tip, with $K_I = 0.64K_{th}^G$ and 3 at.% Re addition in the whole crack system. The pink circles mark the positions of the Re atoms. (a–c) represent the energy differences in the lower atomic layer before, near, and past the saddle-point state in that order; similarly, (d–f) represent the energy differences in the upper atomic layer. (For interpretation of the references to color in this figure legend, the reader is referred to the web version of this article.)

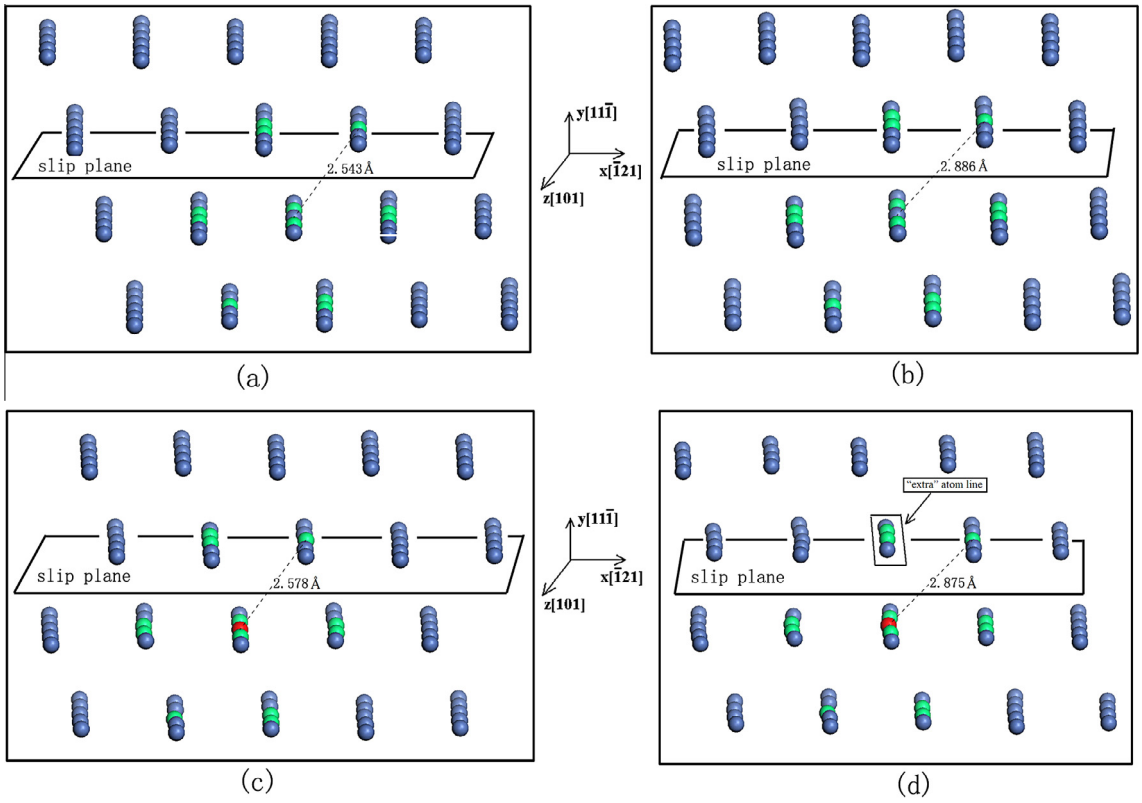

Fig. 11. Several atomic layers across the $(1\,1\,\bar{1})$ slip plane generated in calculating ΔE_{dis} at $K_I = 0.64K_{th}^G$. Red and blue balls represent Re and Ni atoms, respectively. The twelve green balls represent the first nearest-neighbor atoms of Re atom. The configurations are at (a) the initial state without Re addition; (b) the saddle-point state without Re addition; (c) the initial state with a single Re atom in the lower atomic layer of the slip plane; (d) the saddle-point state with a single Re atom in the lower atomic layer. (For interpretation of the references to color in this figure legend, the reader is referred to the web version of this article.)

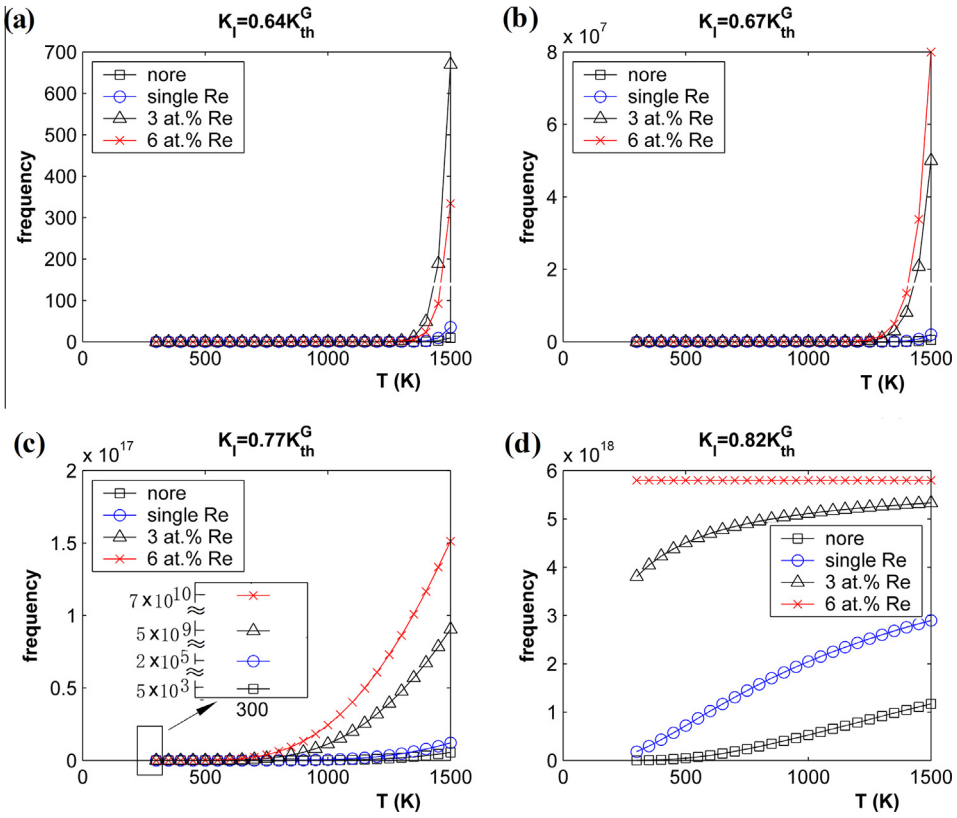

Fig. 12. The curves of dislocation nucleation frequency (ν) versus temperature, without Re and with Re. (a), (b), (c), and (d) represent the curves at $K_I = 0.64K_{th}^G$, $K_I = 0.67K_{th}^G$, $K_I = 0.77K_{th}^G$, and $K_I = 0.82K_{th}^G$, respectively.

are lower compared with the energy differences of atoms far from Re atoms; in Fig. 10(e), in the upper atomic layer of slip plane near the saddle-point state, the energy differences of atoms near Re atoms change little compared with the energy differences of atoms far from Re atoms. This indicates that the overall energy differences for both Re atoms and atoms (near Re atom) in both the lower and upper atomic layers decrease, when the dislocation loop passes Re atoms.

Besides, it is found in the present work that the above conclusion holds up even though Re–Re atomic pairs occur in the lower and upper atomic layers. This indicates that the above conclusion is not influenced by the random locations of Re atoms. Thus, the overall energy differences of Re atom and atoms (near Re atom) decrease when the Re atoms are randomly doped in the whole system. That means that ΔE_{dis} should decrease with the random addition of some concentrated Re (for example, 3 at.% or 6 at.% Re).

The decrease in energy difference of both the Re atom and atoms (near a Re atom) may be related to the local structure expansion around the Re atom during dislocation nucleation.

Fig. 11 shows several atomic layers across the $(1\,1\,\bar{1})$ slip plane at the initial and saddle-point states generated in calculating ΔE_{dis} at $K_I = 0.64K_{th}^{G}$, without and with a single Re atom in the lower atomic layer of the slip plane. At the initial state with the addition of Re in the lower atomic layer (Fig. 11(c)), the average distance between the Re atom and the first nearest-neighbor atoms increases by 0.044 Å compared with the average distance in FCC Ni (Fig. 11(a)), causing a distortion through the volume mismatch between the Re and Ni atoms. At the saddle-point state (Fig. 11(d)), when the dislocation goes through the Re atom, the average distance between the Re atom and the first nearest-neighbor atoms increases by 0.052 Å compared with the average distance at the initial state (Fig. 11(c)), expanding the local structure around the Re atom.

The expanded local structure may be induced by the dislocation core effect. In the dislocation core, there is an "extra" atom line on the top half of the slip plane (Fig. 11(d)), causing the vacancy in the dislocation core, and the local structure around Re atom expands. Fig. 11(d) shows the vacancy in dislocation core. In Fig. 11(d), the distance (2.875 Å) between Re and one of the first nearest-neighbor atoms is longer due to the vacancy in dislocation core, compared with the distance (2.578 Å) in Fig. 11(c).

The expanded structure at the saddle-point state relaxes the volume mismatch (between the Re and Ni atoms) produced at the initial state, causing the energy of both Re atom and atoms (near Re atom) at the saddle-point state to decrease compared with the energy at the initial state (Fig. 11(c)), although the energy of the atoms in the dislocation core should increase due to the distorted structure. Thus, the energy differences for both the Re atom and atoms (near Re atom) in the lower atomic layer decrease.

When Re atom is in the upper atomic layer of slip plane, the "extra" atom line on the top half of the slip plane can tighten the local structure around Re atom, and the local structure around Re atom is not found to expand, and the dislocation core effect does not appear for Re atom. Thus, the energy differences for both the Re atom and atoms (near Re atom) in the upper atomic layer should not decrease.

It is noticed that, only when the dislocation passes the Re atom, the volume mismatch (between the Re and Ni atom at initial state) can be relaxed by the local structure expansion (around the Re atom at saddle-point state), and the energy difference of both Re atom and atoms (near Re atom) decrease. Both the volume mismatch at initial state and the local structure expansion at saddle-point state lead to the decrease of the energy difference of both Re atom and atoms (near Re atom).

3.3. Influence of Re on the nucleation frequency of dislocation

The nucleation frequency (ν) of dislocation can be calculated using the following equation [8]:

$$\nu = n(c/b)\exp[-\Delta E_{dis}/(\kappa T)], \tag{3}$$

where ν is the frequency of spontaneous nucleation events per unit distance along the crack front, n number of nucleation sites per unit length of crack front, set at $n = 1/(36\text{ Å}) \approx 1/(25\,b)$ (here, 25 b is used based on the lateral spread of the dislocation loop along the crack front), $c = 3$ km/s shear wave speed, κ Boltzmann's constant, and T temperature. Assuming that $\nu = 10^6/(\text{mm} \bullet \text{s})$ is the threshold for

Table 2
Peierls stress (σ_p) with and without Re addition.

	0 at.% Re	A single Re atom (in dislocation line)	A single Re atom (ahead of dislocation line)	3 at.% Re	6 at.% Re
σ_p (MPa)	1180	1180	1180	1160	1060

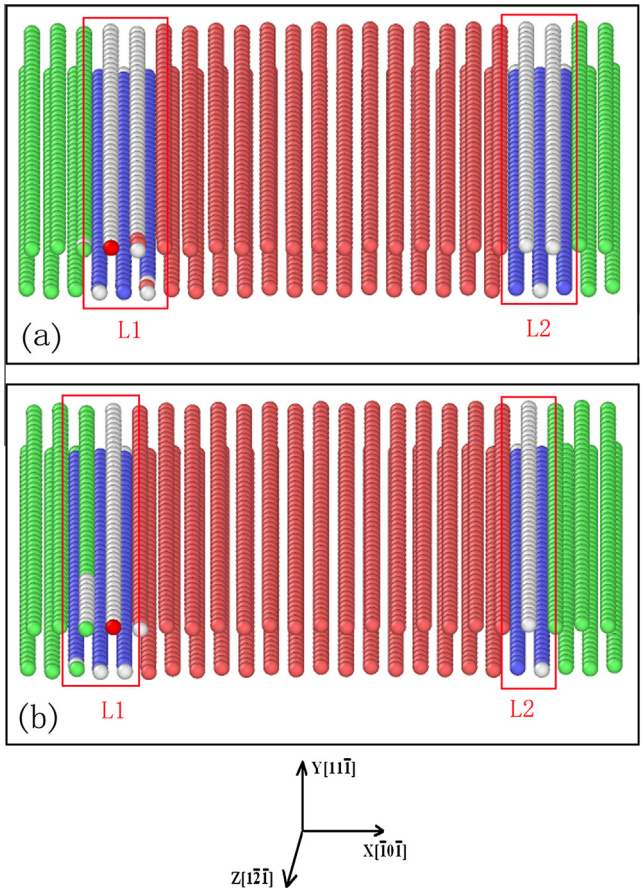

Fig. 13. The configurations of two Shockley partial dislocations with a single Re atom addition, before and after the critical movement of dislocations. The red square frame "L1" and "L2" represent the dislocation cores with Burgers vectors $b_1 = a_0/6[\bar{1}\,\bar{1}\,2]$ and $b_2 = a_0/6[\bar{2}\,1\,\bar{1}]$, respectively. The red ball in the red square frame "L1" represents the Re atom. Green, light red, blue, and, white balls represent the face-centered-cubic (FCC), hexagonal closed-packed (HCP), body-centered cubic (BCC), and unknown structure atoms, respectively. (a) The configurations of dislocations (under 1160 MPa) before the critical movement of dislocations; (b) the configurations of dislocations (under 1180 MPa) after the critical movement of dislocations. (For interpretation of the references to color in this figure legend, the reader is referred to the web version of this article.)

spontaneous nucleation on a laboratory time scale for metals [8], the effect of Re on the dislocation nucleation under external loading can be evaluated using Eq. (3).

Substituting ΔE_{dis} into Eq. (3), v can be obtained. The curves of v versus temperature are depicted in Fig. 12. It can be seen from Fig. 12 that v improves obviously when Re concentration increases. For example, in Fig. 12(b), at 1500 K with $K_I = 0.67K_{th}^G$, $v = 5 \times 10^5$/(mm • s) in pure Ni and $v = 2 \times 10^6$/(mm • s) with the single Re addition, and v exceeds the spontaneous nucleation threshold $v = 10^6$/(mm • s) with the addition of a single Re atom; in Fig. 12(c), at 300 K with $K_I = 0.77K_{th}^G$, $v = 5 \times 10^3$/(mm • s) in pure Ni and $v = 5 \times 10^9$/(mm • s) with the addition of 3 at.% Re, and v exceeds the spontaneous nucleation threshold $v = 10^6$/(mm • s) with the addition of 3 at.% Re. Here, the calculated results of v at 1500 K and 300 K are analyzed because both 1500 K (high temperature) and 300 K (room temperature) are the possible work temperatures for Ni-based single-crystal superalloys.

Therefore, the ductility of the crack in Ni can be enhanced by the addition of Re since the increase of v due to Re addition can exceed the spontaneous nucleation threshold $v = 10^6$/(mm • s) for metals.

3.4. Peierls stress with and without Re addition

Table 2 lists the calculated results of Peierls stress (σ_p) corresponding to the addition of 0 at.%, single Re atom, 3 at.%, and 6 at.% Re. In Table 2, σ_p has not been found to change with single Re atom addition. When Re concentration rises to 3 at.% or 6 at.%, σ_p decreases. For example, σ_p decreases from 1180 MPa to 1060 MPa with 6 at.% addition, comparing with σ_p with 0 at.% Re addition. It can be seen from Table 2 that σ_p decreases when the Re concentration increases. It implies that the trend effect of Re on dislocation mobility is consistent with that on the energy barrier of dislocation nucleation from crack tip, and Re doesn't servers as an obstacle for dislocation motion in the present work.

Fig. 13 shows the configurations of two Shockley partial dislocations with a single Re atom addition, before and after the critical movement of dislocations. Fig. 13 is drawn by the program package Ovito [28]. In Fig. 13, it is not found that the dislocation movement is blocked by Re atom.

4. Conclusions

In the present work, the influence of Re on the activation energy and the frequency of dislocation nucleation from crack tip is investigated. The following conclusions are drawn:

(1) The activation energy of dislocation nucleation decreases with the addition of Re, especially with 3 and 6 at.% Re additions. The decrease may be related to the expansion of local structure around the Re atom when dislocation goes through the Re atom. This expansion relaxes the volume mismatch between the Re and Ni atoms.

(2) The frequency of dislocation nucleation at 300 or 1500 K is improved significantly with the addition of Re, especially with 3 and 6 at.% Re additions; spontaneous dislocation nucleation should be seen on a laboratory time scale. That means the ductility of crack in Ni may be enhanced by Re.

Acknowledgments

The authors would like to thank Jun-Ping Du for helpful discussions. This work was supported by the National Basic Research Program of China (Grant No. 2011CB606402) and the National Natural Science Foundation of China (Grant No. 51071091). Simulations were performed on the "Explorer 100" cluster system of Tsinghua National Laboratory for Information Science and Technology, Beijing, China.

References

[1] E.N. Kablov, N.V. Petrushin, Superalloys 2008, in: R.C. Reed, K.A. Green, P. Caron, T.P. Gabb, M.G. Fahrmann, E.S. Huron, S.A. Woodard (Eds.), TMS, Warrendale, PA, 2008, p. 901.
[2] J.J. Yu, G.C. Hou, N.R. Zhao, T. Jin, X.F. Sun, H.R. Guan, Z.Q. Hu, Rare Met. Mater. Eng. 35 (2006) 1231–1234.
[3] S. Walston, A. Cetel, R. MacKay, K. O'Hara, D. Duhl, R. Dreshfield, Superalloys 2004, in: K.A. Green, T.M. Pollock, H. Harada, T.E. Howson, R.C. Reed, J.J. Schirra (Eds.), TMS, Warrendale, PA, 2004, p. 15.
[4] F. Schubert, T. Rieck, P.J. Ennis, Superalloys 2000, in: T.M. Pollock, R.D. Kissinger, R.R. Bowman, K.A. Green, M. McLean, S. Olson, J.J. Schirra (Eds.), TMS, Warrendale, PA, 2000, p. 341.
[5] M.B. Henderson, J.W. Martin, Acta Mater. 44 (1996) 111–126.
[6] M. Ott, H. Mughrabi, Mater. Sci. Eng. A 272 (1999) 24–30.
[7] J.R. Rice, J. Mech. Phys. Solids 40 (1992) 239.
[8] J.R. Rice, G.E. Beltz, J. Mech. Phys. Solids 42 (1994) 333.
[9] Y.W. Zhang, T.C. Wang, Q.H. Tang, J. Phys. D: Appl. Phys. 28 (1995) 748.
[10] B. Hess, B.J. Thijsse, Erik Van der Giessen, Phys. Rev. B 71 (2005) 054111.
[11] T. Zhu, J. Li, S. Yip, Phys. Rev. Lett. 93 (2004) 025503.
[12] P.A. Gordon, T. Neeraj, M.J. Luton, Modell. Simul. Mater. Sci. Eng. 16 (2008) 045006.
[13] P.A. Gordon, T. Neeraj, Acta Mater. 57 (2009) 3091–3100.
[14] G. Xu, A.S. Argon, M. Ortiz, Philos. Mag. A 72 (1995) 415.
[15] G. Henkelman, H. Jonsson, J. Chem. Phys. 113 (2000) 9978.
[16] G. Henkelman, P.B. Uberuaga, H. Jonsson, J. Chem. Phys. 113 (2000) 9901.
[17] Nakano, Comput. Phys. Comm. 178 (2008) 280.
[18] J.P. Du, C.Y. Wang, T. Yu, Modell. Simul. Mater. Sci. Eng. 21 (2013) 015007.
[19] Z.G. Liu, C.Y. Wang, T. Yu, Modell. Simul. Mater. Sci. Eng. 21 (2013) 045009.
[20] Z.G. Liu, C.Y. Wang, T. Yu, Comput. Mater. Sci. 83 (2014) 196–206.
[21] G.C. Sih, H. Liebowitz, Mathematical theories of brittle facture, in: Fracture: An Advanced Treatise, vol. 2, Academic Press, New York, 1968 (Chapter 2).
[22] The primary developers of LAMMPS are Steve Plimpton, Aidan Thompson, and Paul Crozier. http://lammps.sandia.gov has more information about the code and its uses.
[23] A. Mottura, M.K. Miller, R.C. Reed, Superalloys 2008, in: R.C. Reed, K.A. Green, P. Caron, T.P. Gabb, M.G. Fahrmann, E.S. Huron, S.A. Woodard (Eds.), TMS, Warrendale, PA, 2008, p. 891.
[24] A. Mottura, R.T. Wu, M.W. Finnis, R.C. Reed, Acta Mater. 56 (2008) 2669–2675.
[25] R.E. Peierls, Proc. Phys. Soc. 52 (1940) 34.
[26] Vasily V. Bulatov, Wei Cai, Computer Simulations of Dislocations, Computer Simulations of Dislocations, 2006, p. 22.
[27] E. Rodary, D. Rodney, L. Proville, Y. Bréchet, G. Martin, Phys. Rev. B 70 (2004) 054111.
[28] A. Stukowski, Modell. Simul. Mater. Sci. Eng. 18 (2010) 015012. http://ovito.org/ has more information about the code and its uses.